JOURNAL OF VIROLOGY, Dec. 2007, p. 13230–13234 Vol. 81, No. 23
0022-538X/07/$08.00+0 doi:10.1128/JVI.00847-07

NOTES

Monoclonal Antibodies Providing Topological Information on the Duck Hepatitis B Virus Core Protein and Avihepadnaviral Nucleocapsid Structure▽†

Jolanta Vorreiter,[1] Immanuel Leifer,[1] Christine Rösler,[1] Ludmila Jackevica,[2] Paul Pumpens,[2] and Michael Nassal[1]*

University Hospital Freiburg, Internal Medicine 2/Molecular Biology, Hugstetter Str. 55, D-79106 Freiburg, Germany,[1] *and Latvian Biomedical Research and Study Centre, Ratsupites Str. 1, Riga, LV-1067, Latvia*[2]

Received 20 April 2007/Accepted 11 September 2007

The icosahedral capsid of duck hepatitis B virus (DHBV) is formed by a single core protein species (DHBc). DHBc is much larger than HBc from human HBV, and no high-resolution structure is available. In an accompanying study (M. Nassal, I. Leifer, I. Wingert, K. Dallmeier, S. Prinz, and J. Vorreiter, J. Virol. 81:13218–13229, 2007), we used extensive mutagenesis to derive a structural model for DHBc. For independent validation, we here mapped the epitopes of seven anti-DHBc monoclonal antibodies. Using numerous recombinant DHBc proteins and authentic nucleocapsids from different avihepadnaviruses as test antigens, plus a panel of complementary assays, particle-specific and exposed plus buried linear epitopes were revealed. These data fully support key features of the model.

Duck hepatitis B virus (DHBV) is an important model hepadnavirus (4, 14); however, structural knowledge of DHBV is much less advanced than for human HBV (17). With 262 amino acids (aa) in length, the DHBV core protein (DHBc) constituting the nucleocapsid shell is much larger than its ~180-aa HBV counterpart HBc. In the accompanying study (10a) we used a large panel of recombinant DHBc variants to derive a structural model for DHBc (shown there in Fig. 8C). The model predicts, inter alia, that the N-proximal ~185 aa of DHBc, forming the assembly domain, adopt an architecture similar to that of the first 140 aa of HBc and yet with an ~45-aa central insertion (residues 75 to 120). This insertion would be largely exposed on the DHBc spikes seen in low resolution cryo-electron microscopic reconstructions (7).

As yet, no direct proof for the spatial disposition of specific DHBc protein segments is available, except that peptides from six antigenic regions (AR1 to AR6), recognized by sera from DHBV-infected and/or DHBc-immunized ducks, have been suggested as candidates for surface exposure (18). However, their availability on intact capsids could not experimentally be tested. Furthermore, peptides usually mimic only linear but not conformational epitopes which abound on HBV capsids (2, 6).

To independently test the mutagenesis-derived DHBc model, we generated anti-DHBc monoclonal antibodies (MAbs) and characterized their epitopes. Three MAbs (all immunoglobulin G3 [IgG3]; their full names are 20-2-17C, 21-5-10C, and 27-15-12D [here abbreviated as MAbs n1, n2, and n3]) were obtained by immunization of mice with near-native DHBc particles that precipitated in highly pure form from concentrated recombinant preparations upon storage (10a); four additional MAbs were obtained by immunization (Abnova, Taiwan) with a Sarkosyl-solubilized, partly denatured formulation of the same antigen (all IgG1; full/abbreviated names are as follows: 2B9-4F8/d1, 2B9-4E12/d2, 1A6-3E9/d3, and 2E9-4D10/d4). Finally, freshly gradient-purified, nonprecipitated particles were used to generate polyclonal rabbit (termed 12/99) and chicken (ch anti-DHBc) antisera (at Eurogentec, Belgium; Biogenes, Germany).

To address both linear and conformational epitopes, we used as test antigens numerous recombinant DHBc variants carrying local primary sequence alterations with known consequences for the assembly status (10a) and tested their reactivity with the MAbs in four complementary assay formats.

In the first format (native arrays), native bacterial lysates containing the recombinant proteins (as described in the accompanying study [10a]) were streaked directly onto polyvinylidene difluoride membranes, incubated with the antibody in question, and detected by using an appropriate enzyme-conjugated secondary antibody plus a chemiluminescent substrate. Representative examples are shown in Fig. 1A.

In the second format (native agarose gel electrophoresis [NAGE] blots), purified particle-forming variants (mostly class 1 and class 2 mutants; see reference 10a) were subjected to NAGE and subsequently blotted (Fig. 1B). Positive signals suggest that the respective epitopes are exposed on intact particles; a lack of signals indicates that an epitope is either destroyed in a specific variant or is inaccessible from the particle surface.

* Corresponding author. Mailing address: University Hospital Freiburg, Internal Medicine 2/Molecular Biology, Hugstetter Str. 55, D-79106 Freiburg, Germany. Phone and fax: 49-761-270 3507. E-mail: nassal2@ukl.uni-freiburg.de.

† Supplemental material for this article may be found at http://jvi.asm.org/.

▽ Published ahead of print on 19 September 2007.

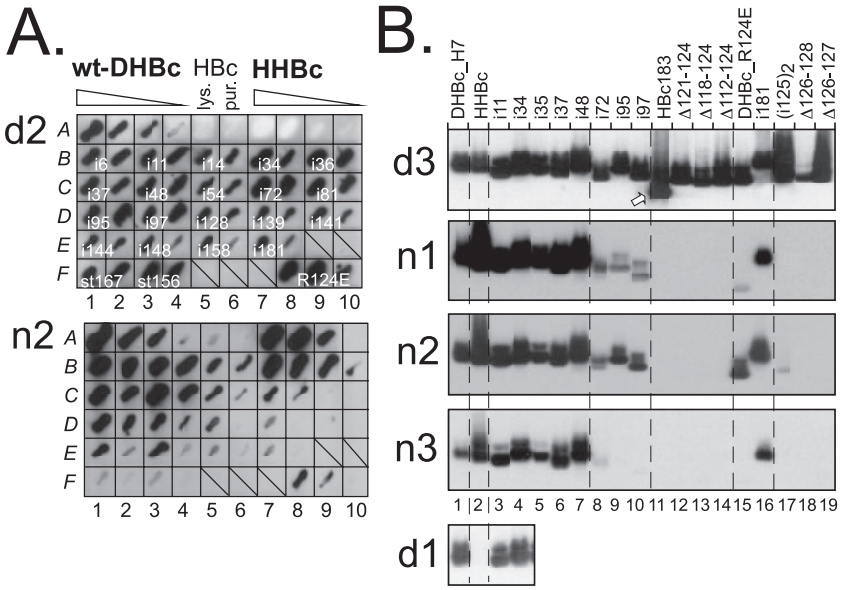

FIG. 1. Distinct reactivities of MAbs against DHBc, DHBc variants, and HHBc on native blots. (A) Native lysate arrays. Sections from arrays probed with MAb d2 and MAb n2 are shown. Aliquots from native bacterial lysates were directly streaked onto the membranes. Blots were developed using a chemiluminescent substrate. Signals were recorded on X-ray film. Fields A1 to A4 and A7 to A10 contained 10-fold dilution series of wt-DHBc and HHBc lysates, starting with about 0.5 μg of antigen. Fields A5 and A6 contained about 3 μg of HBc in lysate or as gradient-purified particles. On the other fields, lysates containing 0.2 to 0.5 μg of the indicated variant proteins were streaked, followed to the right by a 10-fold dilution. Note the strongly different signal intensities, e.g., for HHBc, or the variant with an insertion at position 81 (i81; C9/C10), or the nonassembling variants (st167, F1/F2; st156, F3/F4). (B) NAGE blots. Gradient-purified particles were separated by NAGE, blotted, and immunodetected using the indicated MAbs. The anti-denatured DHBc MAbs, except MAb d4, detected all DHBc antigens; the blot for MAb d3 is shown as an example. The arrow indicates the position of HBc particles visualized by subsequent probing with an anti-HBc MAb. The anti-native MAbs reacted with HHBc and all DHBc variants with peptide insertions between the N terminus and position 48 (i48) and again at position 181 (i181; lane 16). Insertions at position 72 to 97, and the R124E point mutation, differentially reduced recognition; internal deletions (Δ series) prevented detection. The bottom panel illustrates the lack of recognition of HHBc by MAb d1. Tabulary summaries of all antigen-antibody combinations tested are given in Fig. S1 in the supplemental material.

In the third format (sodium dodecyl sulfate-Western blotting [SDS-WB]), total bacterial lysates, obtained by boiling the bacteria in sample buffer and hence containing the antigens in denatured form, were analyzed by SDS-polyacrylamide gel electrophoresis and WB.

In the fourth format (PepScan) antibody reactivity against linear epitopes, represented by 84 filter-immobilized 15-mer peptides (9), each with a 12-aa overlap to the preceding one and covering the entire sequence of DHBc from DHBV3 (16), was tested as previously described (8).

The anti-native DHBc MAbs n1 to n3 reacted poorly or not at all with the denatured antigens, and not with variants with compromised assembly properties (class 3 and class 4 mutants). Most particle-forming variants were well recognized when natively displayed; however, selected mutations (peptide insertions at positions 72, 95, and 97 and the R124E point mutation; short internal deletions around aa 125) caused a strong loss of signal with all three MAbs (Fig. 1B). Hence, these central amino acids contribute importantly to the epitopes of these MAbs.

MAbs d1, d2, and d3 reacted well with all variants in native and denatured form, except for the internal deletion variants Δ82-124 (negative with all three MAbs) and Δ86-124 (negative with d1 and d2; positive with d3). An involvement in epitope formation of the region around aa 82 was confirmed by the PepScan technique, wherein MAb d3 reacted with peptides spanning DHBc residues T64 to P84 and MAbs d1 and d2 reacted with peptides covering P79 to I99. The polyclonal rabbit antiserum 12/99 recognized peptides corresponding to M1 to P36, M67 to Q87, and Y178 to K201. The chicken antiserum reacted with peptides covering M1 to A30, P79 to I99, and I91 to R111 but not with the in-between peptide from G88 to G102, suggesting the existence of two distinct epitopes near position 96.

MAb d4 did not recognize the native forms of most antigens and also reacted extremely weakly with only a single PepScan peptide (R28 to S42). However, in the SDS-WB format it was highly reactive with all variants except i37 and i54 (Fig. 2A); recognition of the in-between insertion variant i48 was only partly reduced. Hence, MAb d4 appeared to recognize a bipartite epitope around position 48 that is buried in intact particles. This was confirmed by testing MAb d4 reactivity against wt-DHBc and the nonassembling variant st167 in the native array format, either without or with SDS treatment of the membrane. Variant st167 was well recognized regardless of SDS treatment, whereas the reactivity of wt-DHBc was at least 10-fold enhanced by prior antigen denaturation (Fig. 2B).

A summary of all mapping data with respect to the primary sequence of DHBc and the core proteins of selected other avihepadnaviruses is shown in Fig. 3.

Final proof for the surface exposure of selected MAb epitopes on intact particles was obtained by testing the ability of the MAbs to coprecipitate the viral genomes present in nucleocapsids of DHBV16 (GenBank accession no. K01834)

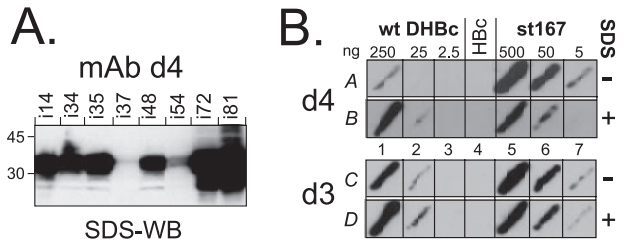

FIG. 2. The epitope of MAb d4 is bipartite and only accessible in nonassembled DHBc. (A) Epitope mapping by SDS-WB of DHBc insertion variants. Similar amounts of various mutant DHBc proteins were analyzed by SDS-WB with MAb d4. All tested peptide insertion variants were well detected except the insertion mutants i37 and i54. A peptide insertion at position 48 (i48) led to an only modest reduction in signal intensity. (B) The MAb d4 epitope is hidden in intact DHBc particles. Aliquots of native lysates containing wt-DHBc and the nonassembling variant st167 were applied in three 10-fold dilutions containing the indicated amounts of antigen; the single HBc control streak contained about 500 ng of core protein. Membrane strip A was directly processed, strip B was first treated for 10 min at 50°C in 0.1% SDS solution. wt-DHBc reactivity was enhanced ~10-fold by SDS treatment (A1 versus B1), whereas st167, if anything, was more efficiently recognized without than with SDS treatment (A5 versus B5). No assembly status-associated differences were detected with MAb d3 (lower panel, fields C and D).

(10) and HHBV-4 (GenBank accession no. M22056) (15) and also of the HBVs of snow geese (SGHBV-15; GenBank accession no. AF110997) (3), storks (STHBV-21; GenBank accession no. AJ251937) (13), cranes (CHBV-2; GenBank accession no. AJ441112) (11), and Ross' geese (RGHBV; GenBank accession no. AY494848) (5). LMH cells were transfected (1) with the cytomegalovirus immediate-early enhancer/promoter-driven DHBV expression vector pCD16 (12) and with homologous constructs for the other avihepadnaviruses. In SDS-WB from aliquots of cytoplasmic lysates of the transfected cells, MAbs d1 and d2 and (weakly) d3 and d4 recognized the DHBV core protein but not the other core proteins, although they were detectable using the polyclonal serum 12/99. Of note, MAb d3 detected in all samples a probably cellular protein with an apparent molecular mass of about 60 kDa (Fig. 4A).

For the nucleocapsid immunoprecipitations, aliquots of each cell lysate were incubated with MAbs n1 to n3 and MAbs d1 to d3 immobilized on protein A-Sepharose. Viral DNAs, liberated by proteinase K treatment, were analyzed by Southern blotting (1). All MAbs except d3 efficiently coprecipitated the typical DNA forms of the DHBV genome; the weak d3 signals were most likely caused by the limited affinity of this MAb, as indicated by admixing recombinant DHBc into the lysates and subsequent WB (results not shown). Efficient precipitation of the other avihepadnavirus DNAs was observed only with the anti-native DHBc MAbs (Fig. 4B and see Fig. S2 in the supplemental material) and with the polyclonal serum 12/99 (Fig. 4C). The DNA patterns from immunoprecipitated samples were not significantly different from that obtained by nuclease treatment of the lysates (1), suggesting that the antibodies did

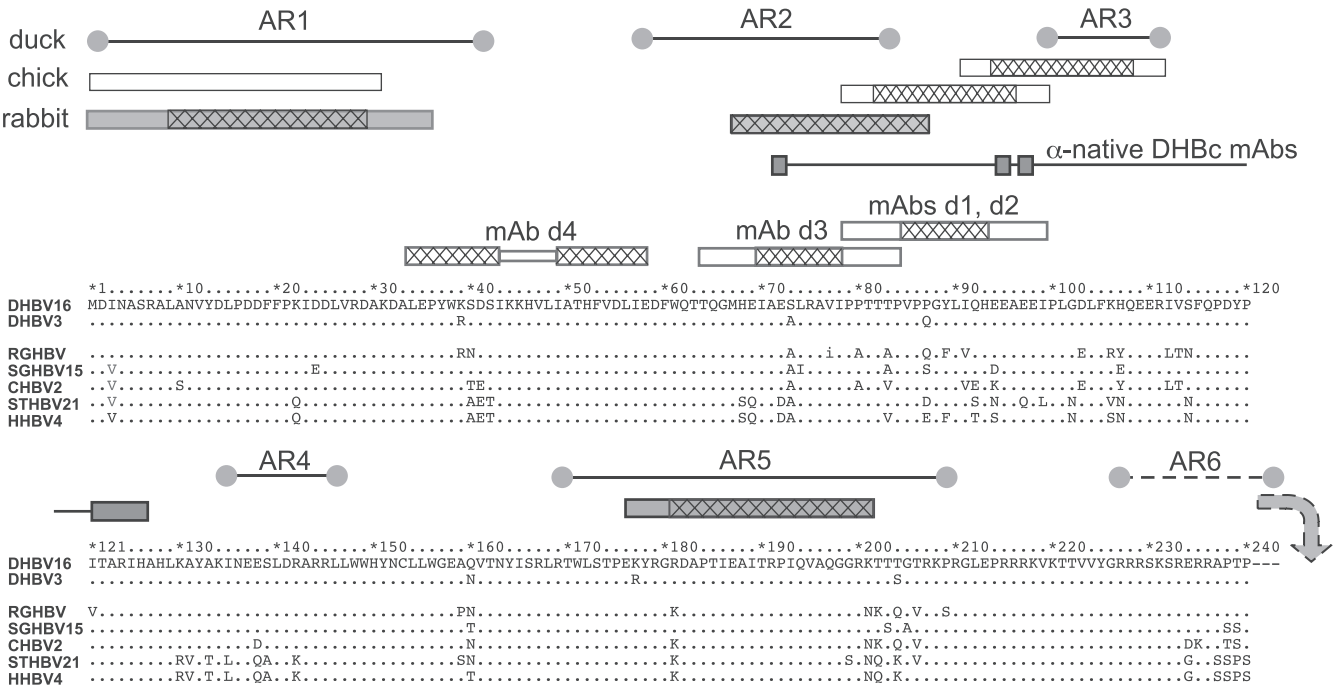

FIG. 3. Epitope locations in the primary sequence of DHBc aligned with other avihepadnaviral core proteins. For DHBV16 core protein, the full sequence is shown, except for the C-terminal residues 241 to 262. Identical amino acids in the other proteins are designated by dots. The boxes above the sequence depict, from bottom to top, the epitopes of the anti-denatured DHBc MAbs and of polyclonal rabbit (dark) and chicken (light) anti-DHBc sera. For PepScan-mapped MAb epitopes, the cross-hatched areas refer to the common core sequence of the recognized peptides. For the polyclonal sera, cross-hatching indicates peptides that gave stronger signals. At the top, the previously reported linear antigenic regions (AR1 to AR6) recognized by duck antisera (18) are shown. AR6 is downstream of DBHc aa 240. The connected rectangles labeled "anti-native DHBc MAbs" show the sites where sequence modifications reduced recognition by these MAbs but not particle formation.

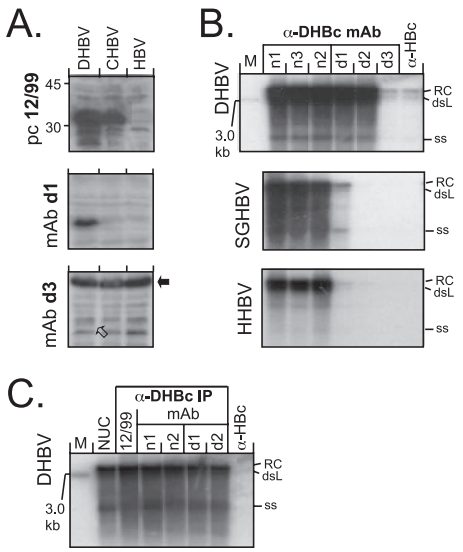

FIG. 4. Reactivity of anti-DHBc MAbs with denatured avihepadnaviral core proteins and native, authentic nucleocapsids. (A) SDS-WB analysis of crude cytoplasmic lysates. Aliquots (5 μl) of cytoplasmic lysates from transfected LMH cell were directly analyzed by SDS-WB and probed with the different antibodies. As examples, blots of lysates from cells transfected with vectors for DHBV, CHBV, and HBV as a negative control and probed with the indicated antibodies are shown. MAb d3 gave only a weak signal at the DHBc position (open arrow) but strongly cross-reacted with a cellular protein of ~60 kDa (black arrow). CHBV core protein was detectable by serum 12/99 but by neither MAb. (B) Southern blot of nucleocapsid-borne avihepadnaviral genomes coprecipitated by anti-DHBc MAbs. Viral DNAs isolated from cytoplasmic nucleocapsids immunoprecipitated by the indicated antibodies were detected by using a ^{32}P-labeled DHBV probe. Results similar to those shown for HHBV and SGHBV were obtained with RGHBV, STHBV, and CHBV (see Fig. S2 in the supplemental material). The positions of the relaxed circular (RC), double-stranded linear (dsL), and single-stranded (ss) DNA forms are indicated. M, linear 3.0-kb marker DNA fragment. (C) Anti-DHBc MAbs recognize differently matured DHBV nucleocapsids with similar efficiency. Nucleocapsid-associated viral DNAs from transfected cells were isolated by either by nuclease treatment (1) of cytoplasmic lysates (lane NUC) or by immunoprecipitation with either the polyclonal antiserum 12/99 or the indicated MAbs and then analyzed by Southern blotting as in panel B. No significant differences in the ratios of the different DNA forms were observed.

not discriminate between DHBV nucleocapsids containing genomes at different stages of maturation (Fig. 4C).

In conclusion, this combination of data allows specific statements on the topological features of DHBc (superimposed on the structure model [see Fig. 8C in reference 10a]). MAb d1 and d2 epitopes are linear and centered around residues P84 to H93. Because this region was recognized on both recombinant and authentic DHBc capsids, it must be surface exposed, as predicted. The epitope of MAb d3 is also linear and centered around residues I70 to I78. Although the nucleocapsid immunoprecipitation data call for a cautious interpretation, efficient recognition of the epitope on recombinant DHBc particles suggests its surface exposure, a finding consistent with the predicted location at the tip of helix Dα3. The epitopes of all three anti-native DHBc MAbs are conformational and dependent on a multisubunit structure, preventing direct primary sequence assignments. However, the selective abrogation of MAb recognition by mutations that do not per se impair particle assembly still identified specific regions involved in epitope formation, namely, around E72, E95 and E97, and R124. Hence, most of the entire region is probably located on the capsid surface. Of note, natural sequence variation between different avihepadnaviruses (Fig. 3) had no measurable impact on recognition by the anti-native DHBc MAbs, indicating that the overall structure of the capsid surface is highly conserved. The epitope of MAb d4, finally, was accessible only in isolated subunits, a finding consistent with the predicted location of the involved residues at the inner capsid face. Moreover, in HBc residues 42 and 52 pack against each other, connected through a turn involving residues 45 to 48 (19); the corresponding DHBc residues are 41 and 54 and residues 44 to 47. Thus, preservation of this element can easily explain why peptide insertions at DHBc position 37 and 54, but much less so at position 48, had a negative impact on MAb recognition.

The presence of epitopes for the polyclonal anti-DHBc sera between positions 70 and 110, concordant with AR2 and AR3 (18), further supports the surface exposure of this region. The reactivity with peptides derived from residues 1 to 35 and residues 180 to 200, concordant with AR1 and AR5 (18), at least suggests that these regions are also surface accessible. In summary, therefore, these epitope mapping data strongly support key topological features of the proposed DHBc model. In addition, the new MAbs should be useful tools for further structural and functional studies of DHBV and other avihepadnaviruses.

This study was supported by a grant from the Deutsche Forschungsgemeinschaft (DFG Na154/9-1/2).

We are grateful to H. Will, H. Sirma, and D. D. Loeb for providing cloned genomes of various avihepadnaviruses.

REFERENCES

1. **Beck, J., M. Vogel, and M. Nassal.** 2002. dNTP versus NTP discrimination by phenylalanine 451 in duck hepatitis B virus P protein indicates a common structure of the dNTP-binding pocket with other reverse transcriptases. Nucleic Acids Res. **30:**1679–1687.
2. **Belnap, D. M., N. R. Watts, J. F. Conway, N. Cheng, S. J. Stahl, P. T. Wingfield, and A. C. Steven.** 2003. Diversity of core antigen epitopes of hepatitis B virus. Proc. Natl. Acad. Sci. USA **100:**10884–10889.
3. **Chang, S. F., H. J. Netter, M. Bruns, R. Schneider, K. Frolich, and H. Will.** 1999. A new avian hepadnavirus infecting snow geese (*Anser caerulescens*) produces a significant fraction of virions containing single-stranded DNA. Virology **262:**39–54.
4. **Funk, A., M. Mhamdi, H. Will, and H. Sirma.** 2007. Avian hepatitis B viruses: molecular and cellular biology, phylogenesis, and host tropism. World J. Gastroenterol. **13:**91–103.
5. **Guo, H., W. S. Mason, C. E. Aldrich, J. R. Saputelli, D. S. Miller, A. R. Jilbert, and J. E. Newbold.** 2005. Identification and characterization of avihepadnaviruses isolated from exotic anseriformes maintained in captivity. J. Virol. **79:**2729–2742.
6. **Harris, A., D. M. Belnap, N. R. Watts, J. F. Conway, N. Cheng, S. J. Stahl, J. G. Vethanayagam, P. T. Wingfield, and A. C. Steven.** 2006. Epitope diversity of hepatitis B virus capsids: quasi-equivalent variations in spike epitopes and binding of different antibodies to the same epitope. J. Mol. Biol. **355:**562–576.
7. **Kenney, J. M., C. H. von Bonsdorff, M. Nassal, and S. D. Fuller.** 1995. Evolutionary conservation in the hepatitis B virus core structure: comparison of human and duck cores. Structure **3:**1009–1019.
8. **König, S., G. Beterams, and M. Nassal.** 1998. Mapping of homologous interaction sites in the hepatitis B virus core protein. J. Virol. **72:**4997–5005.
9. **Kramer, A., and J. Schneider-Mergener.** 1998. Synthesis and screening of peptide libraries on continuous cellulose membrane supports. Methods Mol. Biol. **87:**25–39.
10. **Mandart, E., A. Kay, and F. Galibert.** 1984. Nucleotide sequence of a cloned duck hepatitis B virus genome: comparison with woodchuck and human hepatitis B virus sequences. J. Virol. **49:**782–792.

10a. **Nassal, M., I. Leifer, I. Wingert, K. Dallmeier, S. Prinz, and J. Vorreiter.**

2007. A structural model for duck hepatitis B virus core protein derived by extensive mutagenesis. J. Virol. **81:**13218–13229.
11. **Prassolov, A., H. Hohenberg, T. Kalinina, C. Schneider, L. Cova, O. Krone, K. Frolich, H. Will, and H. Sirma.** 2003. New hepatitis B virus of cranes that has an unexpected broad host range. J. Virol. **77:**1964–1976.
12. **Protzer, U., M. Nassal, P. W. Chiang, M. Kirschfink, and H. Schaller.** 1999. Interferon gene transfer by a hepatitis B virus vector efficiently suppresses wild-type virus infection. Proc. Natl. Acad. Sci. USA **96:**10818–10823.
13. **Pult, I., H. J. Netter, M. Bruns, A. Prassolov, H. Sirma, H. Hohenberg, S. F. Chang, K. Frolich, O. Krone, E. F. Kaleta, and H. Will.** 2001. Identification and analysis of a new hepadnavirus in white storks. Virology **289:**114–128.
14. **Schultz, U., E. Grgacic, and M. Nassal.** 2004. Duck hepatitis B virus: an invaluable model system for HBV infection. Adv. Virus Res. **63:**1–70.
15. **Sprengel, R., E. F. Kaleta, and H. Will.** 1988. Isolation and characterization of a hepatitis B virus endemic in herons. J. Virol. **62:**3832–3839.
16. **Sprengel, R., R. Schneider, P. L. Marion, D. Fernholz, G. Wildner, and H. Will.** 1991. Comparative sequence analysis of defective and infectious avian hepadnaviruses. Nucleic Acids Res. **19:**4289.
17. **Steven, A. C., J. F. Conway, N. Cheng, N. R. Watts, D. M. Belnap, A. Harris, S. J. Stahl, and P. T. Wingfield.** 2005. Structure, assembly, and antigenicity of hepatitis B virus capsid proteins. Adv. Virus Res. **64:**125–164.
18. **Thermet, A., M. Robaczewska, C. Rollier, O. Hantz, C. Trepo, G. Deleage, and L. Cova.** 2004. Identification of antigenic regions of duck hepatitis B virus core protein with antibodies elicited by DNA immunization and chronic infection. J. Virol. **78:**1945–1953.
19. **Wynne, S. A., R. A. Crowther, and A. G. Leslie.** 1999. The crystal structure of the human hepatitis B virus capsid. Mol. Cell **3:**771–780.